Comparison of Ray-Tracing and Reverse Monte-Carlo Methods: Application to GEO orbit

Rémi Benacquista, Pierre Pourrouquet, Athina Varotsou, Renaud Mangeret, Catherine Barillot, Giovanni Santin and Hugh Evans

***Abstract*— Ray-Tracing and Reverse Monte-Carlo are the two most widely used methods to estimate the dose at component level for space applications. The Ray-Tracing method is fast but presents intrinsic limitations while the Reverse Monte-Carlo method is more precise but more time consuming. In the frame of the ESA GTREFF project, a statistical comparison between these two methods has been performed, based on realistic satellite models for GEO orbit and using FASTRAD®. Results are presented and analyzed.**

***Index Terms*— FASTRAD, Radiation effects, Ray-Tracing, Reverse Monte-Carlo, Total Ionizing Dose**

I. Introduction

In the frame of a space project preparation, possible effects of the space radiation environment on the satellite electronics need to be considered. Concerning Total Ionizing Dose (TID) effects, simulations can be performed on a detailed 3D model including the satellite platform, equipment and electronics. The radiation environment of the mission is used as input and for the dose calculation, two methods are most commonly used: Ray-Tracing (RT) and Reverse Monte Carlo (RMC). The first one has the advantage of being fast, easy to implement and provides with results whose accuracy is fully acceptable within the actual Radiation Hardness Assurance process deployed by the space industry. This is why it is most often applied at industrial level. Nevertheless, it presents some limitations due to the assumptions made, related to the method itself. The RMC is more precise; however, calculations are longer and a higher expertise is required from the radiation engineer.

During the past decades, several comparisons have been performed between these two methods [1-4]. In general, RT is considered to approach RMC results within an uncertainty range of about 30%. However, most of the time, it gives conservative results. For example, [2] and [3] considered both GEO and LEO orbits. *Calvel et al*. [4], performed a RT/RMC TID comparison on simple and complex models. For complex models, a total of 408 components were considered, distributed inside three units placed in a GEO platform. RT estimates ranged from -55% to more than 100% with respect to the RMC ones.

However, the *Calvel et al*. study was based on simulations including only electrons (and secondary photons). In the frame of the GTREFF ESA project [5][6], calculations have been performed considering primary and secondary electrons, primary protons and secondary photons. As for *Calvel et al*., our simulations were performed for the case of a GEO mission. In this study, a realistic satellite platform was considered, combined with three different equipment units placed at multiple positions in the spacecraft in order to cover as many different configurations as possible and increase the statistics. Our study was entirely performed with the FASTRAD® software [7].

In the next section the two calculation methods, RT and RMC, are presented. Then, the study cases are described in section III. The results of the comparison are presented in section IV and analyzed in more detail in section V.

II. Ray-Tracing and Reverse Monte-Carlo methods

A. Ray-Tracing Method

When the RT method is applied, the dose is estimated on point detectors placed within a Silicon die for each component. The space around each detector is divided into identical angular sectors and for each of them, a ray is shot from the target to the outside. The equivalent Aluminum shielding crossed by each ray is defined and the corresponding dose is deduced based on the dose depth curve of the mission. The total dose received at component level is then obtained by averaging the dose values over all sectors.

Some important assumptions are made with the RT method:

Manuscript received April 15, 2019. This work was supported by ESA under Contract 4000111684/14/NL/AK.

R. Benacquista and A. Varotsou are with TRAD, Labège, France (phone: +33 5 61 00 95 60; fax: +33 05 61 00 95 61; e-mail: remi.benacquista@trad.fr).

P. Pourrouquet was with TRAD, Labège, France. He is now with Thales Alenia Space, Cannes, France (e-mail: pierre.pourrouquet@thalesaleniaspace.com).

R. Mangeret is with Airbus, in Toulouse, France (e-mail: renaud.mangeret@airbus.com).

C. Barillot is with Thales Alenia Space, Toulouse, France (e-mail: catherine.barillot@thalesaleniaspace.com).

G. Santin and H. Evans are with ESA/ESTEC, Noordwijk, The Netherlands (Giovanni.santin@esa.int, hugh.evans@esa.int)

- For crossed materials other than Aluminum, the thickness is scaled by the material density, compared to that of Aluminum.
- Although no particles are simulated, their dose is somehow implicitly assumed to propagate in straight lines. This is realistic for protons and photons but not necessarily for electrons.
- The RT method is not suitable for TID calculation at material level, since it will not properly work for very low thicknesses, for detectors in materials other than Silicon, Gallium Arsenide and a few others and for very heterogeneous shielding configuration. These limitations are partly related to the dose-depth curve limitations.

For this study, the dose depth curve has been calculated using the SHIELDOSE2 module [8] as implemented in the OMERE software [9]. The solid sphere geometry case has been considered, and therefore the SLANT path method was selected for the RT calculations. Concerning the number of sectors, we performed the calculation with 60 polar angles and 120 azimuthal angles, giving a total of 7200 sectors.

B. Reverse Monte-Carlo Method

The RMC method is expected to give more accurate results since it aims at reproducing the physical interactions between particles and matter. With this method, particles are tracked backwards, from the detector to the outside (as opposed to the case of the Forward Monte Carlo (FMC)). The RMC method is much more suitable for calculations in space applications than the FMC method, since the latter necessitates an unaffordable very important computation time to ensure that particles tracked from the external source reach the very small area of the sensitive chip dies. Even though much faster than FMC, the RMC calculation is still more time consuming compared to RT: for a single detector, an RT calculation typically takes less than a second while an RMC one may take up to 30 minutes (estimated with FASTRAD® for the detailed models used in this study, with one computer thread and ensuring a calculation error below 2%).

The RMC method estimates the dose either for volumes either for point detectors, and, instead of the dose-depth curve, the mission particle fluxes/fluences (electrons and protons) are used as input for the simulation. In this study, we used the same point detectors as for the RT calculation. The input particle fluxes/fluences for trapped electrons and solar protons were calculated for a typical GEO orbit scenario using OMERE [9]. Trapped protons at GEO are not considered since, due to their low energy, they cannot reach the sensitive die inside electronics.

For this study, the RMC method developed in FASTRAD® was used, which is based on GEANT-4 physics [10]. Particles considered include primary and secondary electrons, primary protons, and secondary photons. A validation of the FASTRAD® FMC and RMC methods, by comparisons with MCNPX and GEANT4, has been previously published [11].

III. Study cases

In this study, we considered one GEO platform model and three equipment models. All models were provided by Airbus Defence and Space and Thales Alenia Space, in FASTRAD® format. In order to cover as many different geometry configurations as possible, each equipment was placed inside the platform at ten different locations. With a large number of components inside each equipment (52, 73, and 53) this study has finally been performed on a total of 1780 detectors.

Fig. *1* shows a 3D view of the platform model and of the three units. The units are located on the +/- Y panels (i.e. North/South). Inside the equipment, point detectors are defined in the sensitive die of electronic components placed on the two sides of PCBs. Different types of components and packages are included, as listed in TABLE 1 to TABLE 3. Each package is made of different materials characterized by different density, thickness and chemical composition.

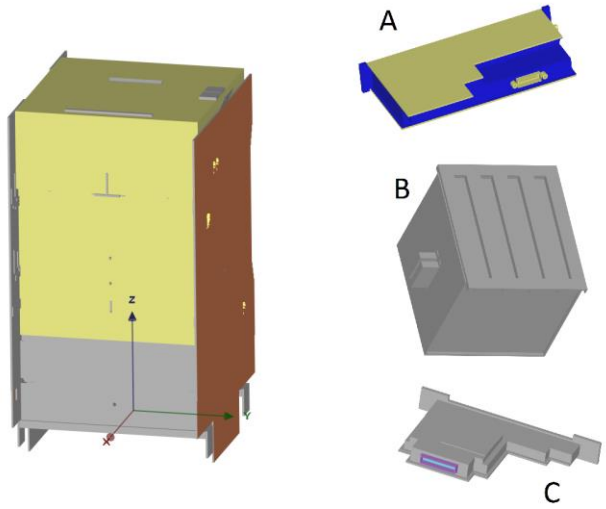

Fig. 1. 3D view of the platform model (on the left) including 10 equipment models at different locations. The units are presented on the right.

TABLE 1
List of Components in unit A

Packages	Quantity
DIL 16	4
Diode	1
Do35	3
FP14	1
MicroX	1
SM1050	31
SOC	1
Thermostat	1
TO18	3
TO39	6
Total	52

TABLE 2
List of Components in unit B

Packages	Quantity
B-Melf	1
SM1050	7
CQFD196	1

D5B	1
D5D	3
FP10	4
FP14	14
FP16	11
FP20	2
HSCV	1
Hbuck	1
Simple Die	4
SOC	9
TO205	4
TO254	4
TO39	1
TO46	2
TO78	2
ZH1	1
TOTAL	73

TABLE 3
LIST OF COMPONENTS IN UNIT C

PACKAGES	QUANTITY
Diode	4
ASIC	1
Simple Die	48
TOTAL	53

IV. CALCULATION RESULTS

Both RT and RMC methods were applied on all 1780 detectors of the three models presented here (one model per unit). The results are summarized in TABLE 4, TABLE 5 and TABLE 6 The first column corresponds to the index of the equipment position. The second column corresponds to the dose range (minimum and maximum values for all detectors of the equipment) calculated with the RMC method. The third column gives the range of RT/RMC dose ratios for all components at each equipment position and the last column gives the percentage of detectors for which this ratio is below 1 (i.e. the RT method underestimates the dose with respect to RMC).

First, it can be seen that the dose ranges (and in particular, the maximum dose value) vary strongly with the units and their position. This was expected, since some of the units are only separated from the outside by the MLI layer while others are stacked between other units and panels. In addition, the unit B (TABLE 5) is more massive that the other, so the calculated doses are lower.

The RT/RMC ratios are very similar for all units and positions. In particular, we notice that the minimum value is between 0.7 and 1.1 for all cases (unit and position). Concerning the fractions of the RT/RMC ratios below 1, it can be seen that they are very dependent on the position of the equipment and can vary from 0% up to 31%.

TABLE 4
COMPARISON BETWEEN RT AND RMC CALCULATION METHODS – CASE A

Position	RMC Dose range [krad]	RT/RMC ratio range	Percentage of ratios below 1
1	[6-87]	[0.9-1.8]	8
2	[4-28]	[0.7-2.0]	31
3	[6-119]	[0.9-1.9]	10
4	[8-182]	[0.9-1.9]	6
5	[5-48]	[0.9-2.1]	13
6	[4-32]	[0.7-1.8]	2
7	[4-38]	[0.9-1.7]	15
8	[5-64]	[0.9-1.8]	8
9	[4-72]	[0.9-1.7]	6
10	[5-65]	[0.7-1.8]	6
Total	[4-182]	[0.7-2.1]	10

TABLE 5
COMPARISON BETWEEN RT AND RMC CALCULATION METHODS – CASE B

Position	RMC Dose range [krad]	RT/RMC ratio range	Percentage of ratios below 1
1	[3-25]	[0.8-1.9]	8
2	[3-25]	[0.7-1.7]	12
3	[4-29]	[0.8-1.7]	10
4	[3-17]	[0.9-1.4]	14
5	[3-13]	[0.9-1.5]	7
6	[3-19]	[0.9-1.8]	10
7	[3-10]	[0.9-1.7]	4
8	[3-19]	[0.8-1.6]	14
9	[3-12]	[0.9-1.9]	3
10	[3-16]	[0.9-1.7]	7
Total	[3-29]	[0.7-1.9]	9

TABLE 6
COMPARISON BETWEEN RT AND RMC CALCULATION METHODS – CASE C

Position	RMC Dose range [krad]	RT/RMC ratio range	Percentage of ratios below 1
1	[6-45]	[1.0-2.2]	0
2	[11-182]	[1.0-2.0]	0
3	[10-144]	[0.7-2.1]	9
4	[9-105]	[0.9-1.7]	2
5	[7-81]	[0.8-2.1]	11
6	[7-68]	[1.1-2.2]	0
7	[6-66]	[0.9-2.6]	4
8	[8-108]	[1.1-3.1]	0
9	[7-141]	[0.9-1.9]	4
10	[8-159]	[1.0-2.3]	0
Total	[6-182]	[0.7-3.1]	3

In order to better understand the distribution of the RT/RMC ratios, a histogram is given in Fig. 2. Here, the statistics for all three units are merged. It indicates the percentage of detectors as a function of the RT/RMC ratio. In total, for 92% (1646 out of 1780) of the detectors, the ratio is above 1 (the red dashed line indicates the ratio = 1), meaning that the RT method overestimates the dose with respect to the RMC method. This overestimation mainly ranges from a factor 1 to 2 however it can be as high as a factor of 3.1. The ratio values are below 0.8 in only 0.4% of the cases (8 detectors out of 1780) with a minimum value equal to 0.7.

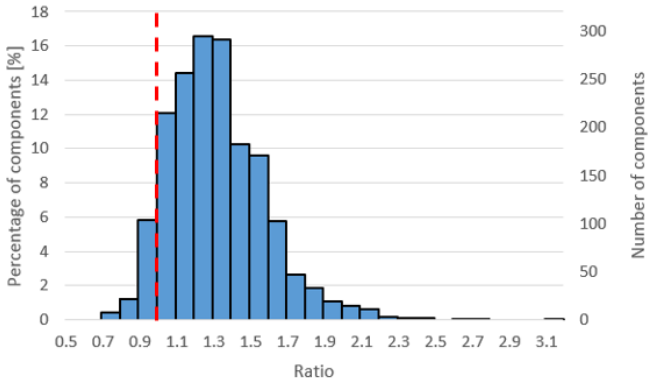

Fig. 2. Histogram of the RT/RMC ratio for all 1780 detectors.

Fig. 3 shows the same distribution of the ratios RT/RMC but distinguishing the different units. While the units A and B display very similar results (despite much lower dose values for unit B, see TABLE 4 and TABLE 5), the results are a bit different for unit C. Indeed, the RT method overestimates the dose value (wrt RMC) for 90% and 91% of the detectors for unit A and B, respectively, and for 97% of the unit C detectors. Since these values are the average for all positions of the units in the platform, it seems that this is due to the unit model only.

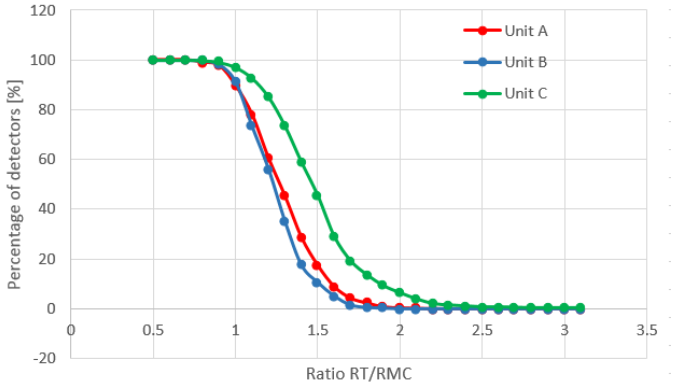

Fig. 3. Cumulative: percentage of components with ratio above a given value.

Fig. 4, Fig. 5, and Fig. 6 give the ratio for all 1780 detectors as a function of the received RMC dose. Each figure corresponds to a unit. The black dashed line indicates a ratio of 1. Note that the scales are not identical. We can observe that the cases with RT/RMC < 1 are mainly located in the dose range between 5 and 20 krad(Si). These cases will be investigated in more detail in the next section.

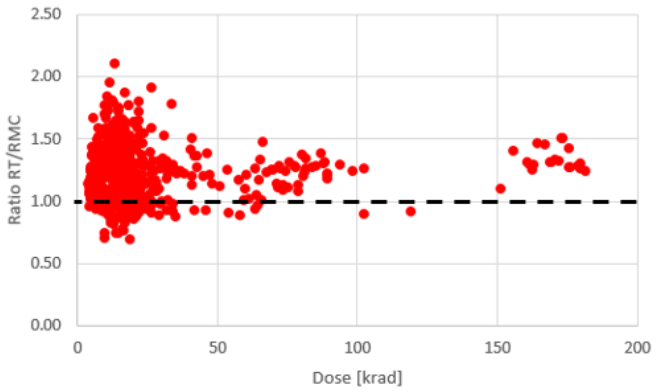

Fig. 4. Ratio as a function of the dose (estimated with RMC) for unit A.

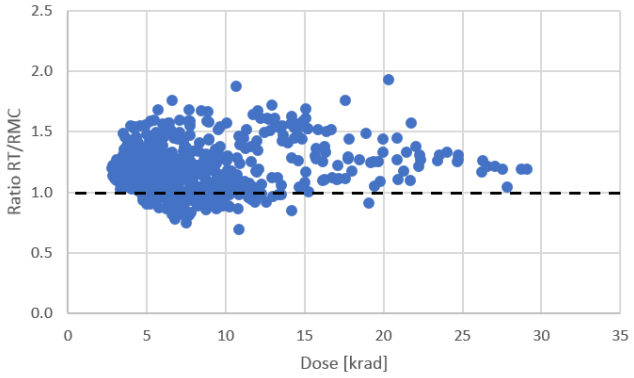

Fig. 5. Ratio as a function of the dose (estimated with RMC) for unit B.

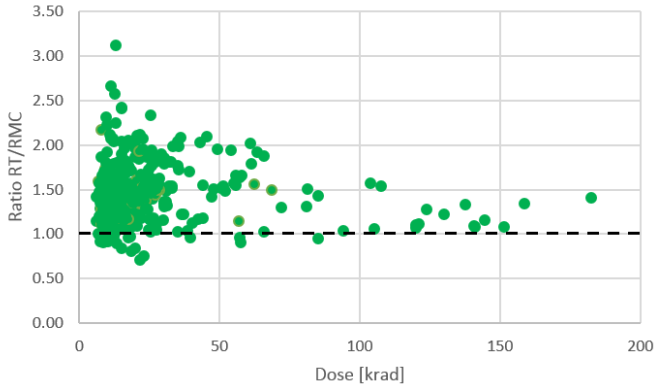

Fig. 6. Ratio as a function of the dose (estimated with RMC) for unit C.

V. Detailed Analysis

In this section, we consider the case of a simple silicon die placed in the unit C at the position 3. For this component, the RT/RMC ratios is one of the lowest (0.71). In order to explain the obtained result, we used the post-processing tools of FASTRAD®.

Fig. 7 shows the post-processing results for both methods. The rays correspond to the RT post-processing and indicate the directions with the "thinnest" shielding (from 2.23mm to 5.39mm). These directions indicate the path of the particles responsible for the higher dose values. In the figure, only 2.3%

of the sectors are displayed but they represent 30% of the total RT dose. The mapping corresponds to the post-processing of the RMC method for this detector. It corresponds to the electron fluence that actually reached the detector. Therefore, it also gives indication on where the dose is mainly coming from.

It can be seen that, for some directions, the two methods have a good agreement: +Y, -Z and +Z (mapping not visible). However, unlike the Ray-tracing, the RMC post-processing predicts that a significant part of the dose also comes from the -X direction.

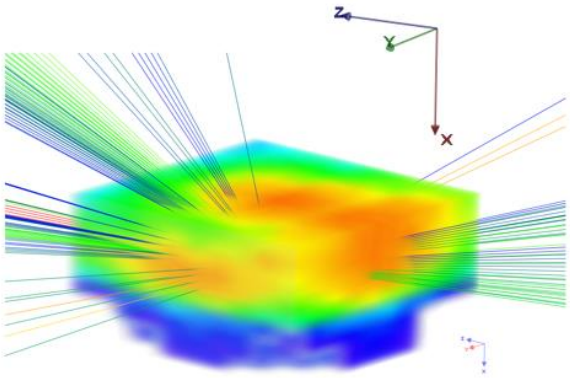

Fig. 7. Post-processing for the RT and RMC calculations in FASTRAD. The rays in color correspond to the directions with the thinnest shielding according to the RT. The color-coded mapping indicates where the electron fluence that reached the detector comes from.

Fig. 8 shows the same post-processing results with the silicon die placed within the unit. The grey box is another unit align with others in the -X direction.

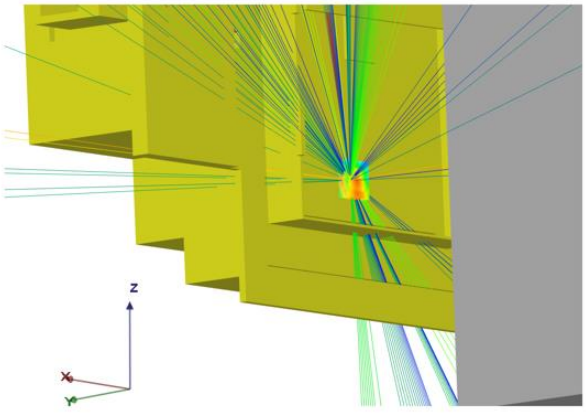

Fig. 8. Post-processing as for figure 7 but here shown inside the equipment and satellite.

According to the RMC calculation and post-processing, a large part of the dose comes from the -X direction. If we consider particles propagating in straight line (ray-tracing) they should have crossed all the units on the -X direction before they reach the silicon die. This is very unlikely since the total thickness crossed in this direction is ~ 20mm (Al).

These particles can either be scattered primary electrons or secondary electrons. Because of their non-linear propagation, the RT method cannot take into account this effect, and the fact that these electrons significantly contributed to the total dose explains the slight RT dose underestimation.

As it can be seen in Fig. 4, Fig. 5 and Fig. 6, the smallest ratios corresponds to a specific dose range, between 5 and 20 krad. The observations made on this section provide part of the explanation. Above this range the dose is predominantly due to primary electrons. For the lowest levels of the dose, photons are expected to be the main contributor. As they do propagate in straight line, the RT method can correctly take them into account and no RT/RMC ratio lower than 1 is found for these dose levels.

VI. Conclusion

A statistical comparison of the dose calculated with Ray-Tracing and Reverse Monte-Carlo was performed in a detailed spacecraft geometry. We considered three realistic equipment units placed at 10 different locations in a realistic satellite model leading to a statistic of 1780 points.

The set of results presented here indicates RT/RMC dose ratios ranging from 0.7 to 3.1. It confirms that RT is conservative in the great majority of tested cases (92%) since only 8% of the components exhibited a ratio smaller than 1. On top of it, among them, less than 6% falls below 0.8, with a minimum value of 0.7.

A first analysis allowed one possible cause of the RT underestimation to be determined, that being the scattered primary electrons and the secondary electrons contributing to the dose.

References

[1] G. Santin. “Radiation Interaction. Physics and Simulation”. RADECS Short Course, chap 2, 2013.

[2] R. Mangeret, “Impact des propriétés effectives des matériaux et structures de blindage sur le calcul de niveaux de dose,” ASTRIUM report AIN.RA.RM.705.102.01, Jan. 2001.

[3] R. Mangeret, “Environment (mission) analysis and specification”, RADECS 2003. Short course notes.

[4] P. Calvel et al., "Review of Deposited Dose Calculation Methods Using Ray Tracing Approximations," in *IEEE* Transactions on Nuclear Science, vol. 55, no. 6, pp. 3106-3113, Dec. 2008.

[5] A. Varotsou et al., “GEO Telecoms Radiation Tools Efficiency Improvement with Methods and Geometry Exchanges for Industrial Tools”, presented at the TEC-EES Final Presentation Days, ESTEC, Noordwjik, Netherlands, October 2016.

[6] A. Varotsou et al., “Six-Faces Induced Margins on Dose Calculation and Proposal for a New Satellite Geometry Exchange method” submitted for presentation at Radiation and its Effects on Components and Systems – RADECS, Montpellier, France, Sept. 2019.

[7] FASTRAD software: http://www.fastrad.net

[8] Stephen M. Meltzer, “Electron, Electron-Bremmstrahlung and Proton Depth-Dose Data for Space Shielding Applications”, IEEE Trans. Nucl. Sci. NS-26, 4896 (1979).

[9] OMERE software: http://www.trad.fr/en/space/omere-software/

[10] S. Agostinelli, et al. “GEANT4-a simulation toolkit”, Nuclear Instruments and Methods in Physics Research, vol. 506, pp. 250-303, Jul. 2003

[11] P. Pourrouquet et al., "Comparative study between Monte-Carlo tools for space applications," 2016 16th European Conference on Radiation and Its Effects on Components and Systems (RADECS), Bremen, Germany, September 2016.